

## Enhancement of induced V polarization due to rough interfaces in polycrystalline V/Fe/V trilayers

C. Clavero,<sup>1</sup> J. R. Skuza,<sup>2</sup> Y. Choi,<sup>3</sup> D. Haskel,<sup>4</sup> C. Sánchez-Hanke,<sup>5</sup> R. Loloee,<sup>6</sup> M. Zhernenkov,<sup>7</sup> M. R. Fitzsimmons,<sup>7</sup> and R. A. Lukaszew<sup>1,2</sup>

<sup>1</sup>*Department of Applied Science, College of William & Mary, Williamsburg, Virginia 23187, USA*

<sup>2</sup>*Department of Physics, College of William & Mary, Williamsburg, Virginia 23187, USA*

<sup>3</sup>*Consortium for Advanced Radiation Sources, University of Chicago, Chicago, Illinois 60637, USA*

<sup>4</sup>*Advanced Photon Source, Argonne National Laboratory, Argonne, Illinois 60439, USA*

<sup>5</sup>*National Synchrotron Light Source, Brookhaven National Laboratory, Upton, New York 11973, USA*

<sup>6</sup>*Department of Physics and Astronomy, Michigan State University, East Lansing, Michigan 48824, USA*

<sup>7</sup>*Los Alamos National Laboratory, Los Alamos, New Mexico 87545, USA*

(Received 16 April 2009; revised manuscript received 18 June 2009; published 20 July 2009)

The effect of interface roughness on the induced polarization of V in polycrystalline V/Fe/V trilayers was investigated with x-ray magnetic circular dichroism, x-ray resonant magnetic scattering, and polarized neutron reflectometry. Trilayer samples were sputter deposited onto Si substrates at room temperature to minimize interdiffusion. The films were polycrystalline and exhibited an average 0.5 nm root-mean-square interfacial roughness at the Fe/V interfaces. The induced polarization found in V was constrained to the Fe/V interface extending approximately up to 2–3 monolayers into the V and exhibited antiferromagnetic alignment to the Fe layer. A magnetic moment for V ranging between  $-0.46$  and  $-0.86 \mu_B/\text{V}$  atom is consistent with the neutron and resonant x-ray data. Notably, this value for structurally rough interfaces is significantly larger than that reported for samples with atomically flat Fe/V interfaces.

DOI: [10.1103/PhysRevB.80.024418](https://doi.org/10.1103/PhysRevB.80.024418)

PACS number(s): 75.70.Cn, 78.70.Dm, 61.05.fj

### I. INTRODUCTION

Proximity effects leading to induced magnetic moments in nonmagnetic thin-film layers in contact with ferromagnetic films have attracted great interest over the last two decades. In the particular case of V, it exhibits a magnetic moment of  $3 \mu_B$  as a single atom in the ground state<sup>1</sup> but bulk body-centered-cubic V does not order magnetically. Nevertheless, V acquires an induced magnetic moment in proximity with a ferromagnetic element. V polarization induced by proximity to Fe has been extensively studied in multilayers grown on MgO(001) (Ref. 2–6) and Cu(100) (Ref. 7) substrates, favoring epitaxial growth with high-quality crystalline structure. In the case of Fe/V multilayers deposited on MgO(001) substrates, reports indicate that within a narrow deposition temperature range, i.e., 573–600 K, high crystal quality with low mosaic spread and sharp interfaces<sup>8,9</sup> with very low interface roughness values ( $\sim 0.1$  nm) were achieved. On the other hand, significant interdiffusion and alloying was found at Fe/V interfaces when the multilayers were deposited at temperatures higher than 600 K.<sup>2,3,8</sup> Scherz *et al.* (Ref. 2) studied the effect of interdiffusion in Fe/V/Fe trilayers grown at room temperature (RT) and 600 K. While no interdiffusion was found for trilayers deposited at RT displaying atomically flat interfaces, the formation of more than one interdiffused layer at the Fe/V interface was observed upon deposition at 600 K, giving rise to a doubling of the magnetic moment of V and also a larger spatial extent of V polarization. Accordingly, a number of experimental and theoretical reports indicate that Fe/V multilayers grown at temperatures lower than 600 K lead to the formation of an abrupt interface without any diffusion in the Fe substrate,<sup>2,10–16</sup> due to the low diffusion coefficient of V. In fact, experimental values for the

diffusion coefficient  $D$  of V in Fe-V solid solutions in the temperature range of 1112–1593 K have been reported and the measured values follow Arrhenius behavior.<sup>17</sup> Extrapolation to RT yields  $D \sim 10^{-41}$  cm<sup>2</sup>/s for such a coefficient implying that diffusion at RT is practically nonexistent.

In general, interdiffusion is understood as interchange of Fe and V atoms across the interface and therefore indistinguishable from interfacial alloying, whereas roughness suggests amplitude variations in the thickness of any given layer without any interchange across it.<sup>3</sup> In order to study the role of roughness or interdiffusion on the induced magnetism of V, it is important to discuss their origin. Interface imperfections can result from a variety of material and/or growth-dependent mechanisms, and in turn can affect dramatically the magnetic properties of the system. In fact during the early research on oscillatory giant magnetoresistance and interlayer exchange studies it was found that growth-induced defects hindered these effects in molecular-beam-epitaxy-grown Co/Cu(111) multilayers while they were fully developed in polycrystalline sputtered multilayers.<sup>18</sup> This behavior was attributed to growth-induced defects arising from twinned islanding in epitaxial growth unlikely to occur in polycrystalline sputtered samples. Polycrystalline interfaces have an intrinsic roughness originating from differences in monolayer step height for different growth orientations. Further, roughness results from low adatom surface mobility and typically dominates for deposition at lower temperatures and therefore samples deposited at RT typically exhibit roughness-dominated interfaces. In fact, this is a reason why ion-beam-assisted deposition is an attractive methodology for multilayer deposition with minimal interlayer diffusion in a wide temperature range.<sup>19</sup>

All the above mentioned reports study the V polarization in atomically flat Fe/V interfaces with different degrees of

interdiffusion. Nevertheless, the isolated effect of roughness (in the absence of interdiffusion) on the induced polarization of V in Fe/V interfaces has not been addressed yet. In order to investigate this point, polycrystalline V/Fe/V trilayered samples were sputter deposited on Si substrates. The films were deposited at RT so that interdiffusion was significantly minimized as discussed above. Furthermore, the substrate and growth conditions used led to polycrystalline films with moderate interfacial roughness of approximately 0.5 nm root mean square (rms). Due to the small magnetic signal of the polarized V arising from both Fe/V interfaces, a combination of complementary experimental techniques, including x-ray reflectometry (XRR), polarized neutron reflectometry (PNR), x-ray magnetic circular dichroism (XMCD), x-ray resonant magnetic scattering (XRMS), and superconducting quantum interference device (SQUID) magnetometry were used in the present study. The film layered structure was characterized using XRR and its magnetic layered structure using PNR. PNR provides chemical and magnetization depth profiles. XMCD and XRMS provide element-specific magnetic information, the latter with depth resolution. SQUID measures the volume-averaged magnetic response. Our results indicate that interfacial roughness significantly enhances the induced V magnetic moment.

## II. EXPERIMENT

V/Fe/V trilayers were grown on Si substrates via dc sputtering deposition in an ultrahigh vacuum system working under a base pressure in the low  $10^{-7}$  Pa. The Fe and V layers were deposited at RT with deposition rates of 0.22 nm/s for V and 0.4 nm/s for Fe. The thicknesses of the layers were chosen to provide a significant fraction of V atoms in close proximity to an interface.<sup>5</sup> After deposition of the trilayer, a 3-nm-thick Au cap layer was immediately deposited at RT and with a rate of 0.4 nm/s to prevent oxidation. The nominal film layer structure was Si/V(2 nm)/Fe(3 nm)/V(2 nm)/Au(3 nm). Atomic force microscopy investigations revealed a granular growth-mode characteristic of polycrystalline films with an in-plane correlation length<sup>20,21</sup> of  $(100 \pm 9)$  nm, which replicates through the different interfaces as a consequence of RT deposition conditions and the consequent low mobility of the incoming adatoms.

XRR measurements were performed *ex situ* using a standard four-circle diffractometer with Cu  $K\alpha$  radiation ( $E = 8.048$  keV) at the x-ray diffraction facilities at LANSCE, Los Alamos National Laboratory. PNR studies were also carried out at LANSCE, using the Asterix polarized beam (polarization  $\sim 93\%$ ) reflectometer/diffractometer with polarization analysis. The neutron measurements were performed in a 0.6 T field at RT. XRMS and XMCD measurements were collected at the National Synchrotron Light Source beamline X13A. This beamline delivers elliptically polarized soft x-rays in an energy range between 200 and 1600 eV. The measurements were performed in a 0.5 T field at RT. The circular polarization component ( $P_c \sim 70\%$ ) is modulated by switching x-ray helicity at frequencies close to 22 Hz. Magnetic circular dichroism (MCD), or the difference in sample absorption measured with left and right circularly polarized

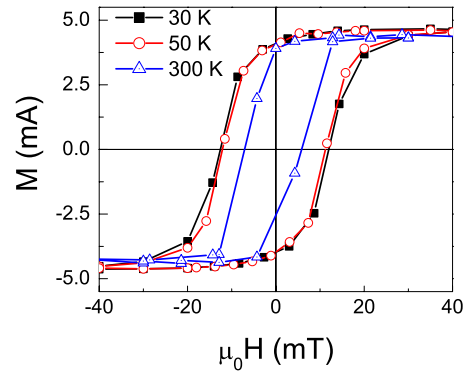


FIG. 1. (Color online) In-plane SQUID loops for the V/Fe/V trilayer measured at 30, 50, and 300 K given in magnetization per unit area units ( $\text{mA} = 10^{-4} \text{ emu/cm}^2$ ).

x-rays, provides element-specific magnetic data. The dc and ac components of the modulated absorption provide simultaneous collection of the absorption and MCD signals, respectively, in a single energy scan. The modulation technique increases the sensitivity for detection of small magnetic signals such as the induced V polarization in the V/Fe/V trilayers. Finally, magnetization measurements were carried out using a SQUID magnetometer at temperatures from 30 K to RT using in-plane magnetic fields intense enough to saturate the sample.

## III. RESULTS

### A. SQUID magnetometry

The magnetization reversal and magnetic anisotropy of the trilayered V/Fe/V sample was studied measuring hysteresis loops at 30, 50, and 300 K with SQUID magnetometry. This technique probes the total magnetization of the system. In-plane magnetic anisotropy is evidenced by the shape of the in-plane hysteresis loops shown in Fig. 1. High in-plane remanence magnetization values close to 100% were obtained whereas a progressive decrease in the coercive field is found as the temperature increases ranging from 6.5 mT at 300 K to 12 mT at 30 K. A 6.5% decrease in the saturation magnetization  $M_s$  per area unit is found at RT compared with lower temperatures with a value of  $(4.3 \pm 0.5)$  mA  $[(4.3 \pm 0.5) \times 10^{-4} \text{ emu/cm}^2]$ . The observed decrease in  $H_c$  and  $M_s$  with increasing temperature is expected for magnetic thin films.<sup>22,23</sup>

### B. XRR

XRR analysis provided a quantitative measure of the thickness and chemical roughness of the different layers in the trilayered films. Figure 2(a) shows the x-ray specular reflectivity normalized by the Fresnel reflectivity ( $R_F = 16\pi^2/q_z^4$ ) obtained using Cu  $K\alpha$  radiation. The high number and the sharpness of the oscillations suggest moderate interfacial roughness. Figure 2(b) shows the scattering length density (SLD) profile (continuous lines) used in the model to produce the solid reflectivity curve in Fig. 2(a), along with the convoluted roughness (CR) SLD profile (dashed lines).

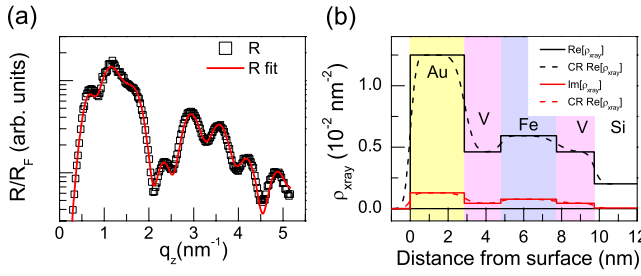


FIG. 2. (Color online) (a) X-ray specular reflectivity normalized by the Fresnel reflectivity  $R_F=16\pi^2/q_z^4$  (dots) and corresponding fitting (line), (b) SLD  $\rho$  profile used for the x ray fitting. Dashed lines show the CR SLD profiles.

The reflectivity curve was calculated using Parratt’s recursive formalism with roughness.<sup>24,25</sup> A measure of goodness-of-fit,<sup>26</sup>  $\chi^2$ , was optimized by perturbing the thickness and roughness parameters of the model. The fits yielded a deviation smaller than 5% from the nominal thickness for all the layers (Table I). The error bar reported in Table I corresponds to the deviation of the parameter that increases fourfold the minimum value of  $\chi^2$  (i.e., a 2- $\sigma$  error bar). The scattering length densities used in the model were fixed to the bulk values as obtained from the literature.<sup>27</sup>

C. XMCD and XRMS analysis

To clarify the extent and magnitude of the V polarization at the Fe/V interfaces, XMCD and XRMS scans were carried out.<sup>28</sup> Element-specific spectra at the  $L_{2,3}$  edges of Fe and V were obtained at different temperatures using fluorescence detection mode. An in-plane magnetic field parallel to the incident x-ray wave vector was applied. Measurements were carried out by switching the helicity of circularly polarized x-rays at each scattering vector and also for opposite directions of the applied field. Since helicity switching is equivalent to magnetization reversal, this allows checking for experimental artifacts. In order to clarify whether or not V is polarized at the Fe/V interfaces, dichroism measurements were performed at the  $L_{2,3}$  Fe and V edges with variable in-plane magnetic fields in order to obtain element-specific hysteresis loops. Figures 3(a) and 3(b) show element-specific hysteresis loops for Fe and V measured at RT. As can be observed, the loops exhibit opposite signs, indicating not only V polarization but also antiferromagnetic coupling be-

TABLE I. Thickness and upper interface roughness from the x-ray specular reflectivity analysis and from the neutrons analysis.

	Thickness (nm)	Upper interface roughness rms (nm) for x-rays	Upper interface roughness rms (nm) for neutrons
<b>Au</b>	$2.86 \pm 0.01$	$0.24 \pm 0.01$	$1.00 \pm 0.04$
<b>V</b>	$1.92 \pm 0.02$	$0.41 \pm 0.01$	$0.64 \pm 0.05$
<b>Fe</b>	$29.5 \pm 0.02$	$0.3 \pm 0.02$	$0.29 \pm 0.03$
<b>V</b>	$2.0 \pm 0.1$	$0.62 \pm 0.04$	$0.6 \pm 0.02$
<b>Si</b>		$0.27 \pm 0.01$	$0.78 \pm 0.14$

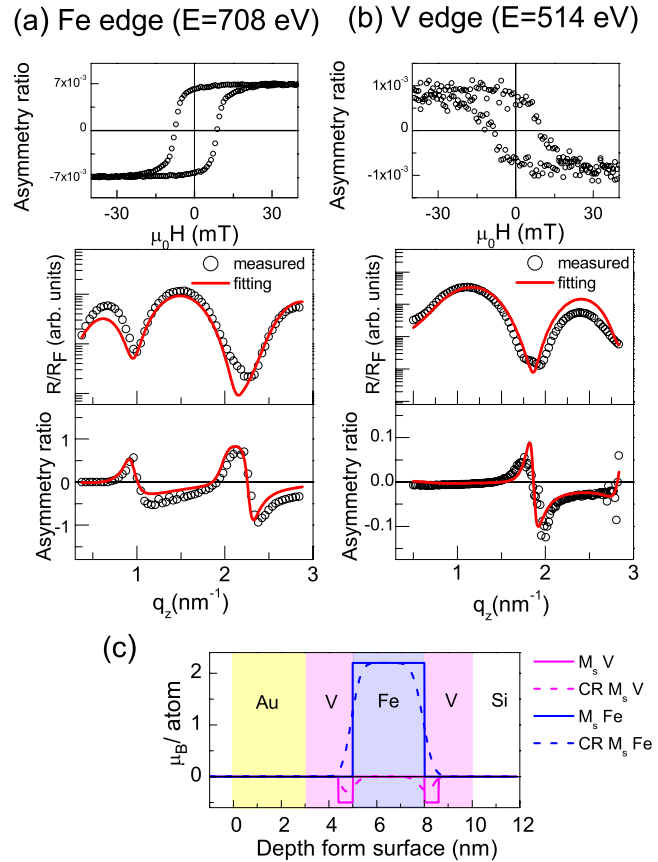


FIG. 3. (Color online) Element-specific hysteresis loops, reflectivity normalized by the Fresnel reflectivity, and asymmetry ratio measured at RT at the (a) Fe and (b) V  $L$  edges. (c) Fe and V SLD profiles considered for the fittings. Dashed lines show the CR SLD and magnetization profiles.

tween Fe and V. It is worth noticing that both elements exhibit the same coercive and saturation fields, indicating Fe and V magnetizations are strongly coupled and directly related, as previously observed in Al/Co/V/MgO(100) multilayers.<sup>29</sup> Furthermore, coercive and saturation fields are compatible with the SQUID observations at RT.

In order to investigate the location and extent of the V polarization, XRMS reflectivity data were obtained at the Fe and V  $L_{2,3}$  edges as a function of the scattering vector  $q_z$ , as shown in Figs. 3(a) and 3(b). Asymmetry ratio curves  $\Delta R = (I^+ - I^-)/(I^+ + I^-)$ , where (+, -) denote opposite x-ray helicity, were obtained in each case. Interestingly, a nonzero asymmetry ratio is found at the V edge, confirming the magnetic polarization of V. It is worth noticing that owing to the low thickness of the films, the x-ray radiation is able to penetrate the V/Fe/V trilayer and to probe both Fe/V interfaces. The scans were fitted using the distorted-wave Born approximation,<sup>30,31</sup> employing structural parameters obtained from XRR (Table I). The imaginary parts of resonant chemical and magnetic scattering factors were obtained from the literature<sup>7</sup> with real parts derived from a differential Kramers-Krönig transform. The interface roughness was modeled using the Nevot-Croce approach.<sup>25</sup> For Fe we used resonant charge and magnetic scattering factors experimentally obtained from a magnetically saturated Fe standard film

whereas for V they were obtained from Ref. 7. Interestingly, in our case the XRMS fitting indicates antiferromagnetically induced V polarization at both Fe/V interfaces, extending approximately 0.6 nm ( $\sim 3$  ML) into the V films, compatible with the rms interfacial roughness. V magnetization is found to be antiparallel to the applied field direction, which is parallel to the Fe magnetization, and this is consistent with the XMCD results. While XRMS does not directly measure magnetization in absolute units but rather yields relative changes in element-specific depth-resolved magnetization, the refined magnetic scattering factors can be placed in absolute magnetization units by comparing with an appropriate standard where the element-specific magnetization is known. As previously mentioned, the magnetic scattering factors used in the V XRMS fits were obtained from Ref. 7, where an induced magnetic moment of  $1.0 \mu_B/\text{V}$  atom was measured on V/Fe multilayers using sum-rules analysis. These magnetic scattering factors needed to be scaled by 0.54 in order to fit the data, resulting in an estimated V magnetic moment per atom in the polarized area of  $(-0.54 \pm 0.15) \mu_B/\text{V}$  atom. Figure 3(c) shows the Fe and V magnetic-moment profiles employed to fit the XRMS curves. The dashed lines show the convoluted roughness magnetization profile. The total saturation magnetization calculated from the XRMS model yields a net saturation magnetization per area unit of  $4.7 \text{ mA}$  ( $4.7 \times 10^{-4} \text{ emu/cm}^2$ ), value within the error bar of the SQUID measurement.

It is worth noticing that in the above mentioned model a reduction in the magnetic moment of Fe at the Fe/V interface was not considered, although this effect was systematically observed in previous reports.<sup>32</sup> Owing to the limited  $q_z$  range and the relatively long wavelength of the incident x-rays, this scenario did not improve significantly the XRMS fits. In addition the use of resonant scattering factors obtained from previous reports<sup>7</sup> adds additional uncertainty. Nevertheless, this point was further investigated with PNR since this method does not share the aforementioned limitations for this particular case, as it will be shown in the next section.

#### D. PNR

PNR is an established method<sup>33–36</sup> to investigate chemical and magnetic profiles in multilayers. In contrast to the element specificity of x-ray-based magnetic techniques, the specular neutron reflectivity is related to the depth dependence of the average magnetization. Both techniques are scattering techniques and thus average information over the lateral dimensions of the sample within the coherence of the x-ray or neutron beam. The experimental reflectivity data for the trilayered V/Fe/V sample normalized by the Fresnel reflectivity are shown in Fig. 4.  $R^{++}$  and  $R^{--}$  correspond to the reflectivity curves measured with the polarization vector of the incident and scattered neutron beams parallel and antiparallel to the external magnetic field, respectively. In contrast to the XRR case, which is only sensitive to the chemical profile of the sample, PNR is sensitive to the nuclear and magnetic depth profiles. For the case of PNR, the SLD  $\rho$  is the atomic number density of scattering centers,  $N$ , times the sum of their nuclear  $b$  and magnetic  $p$  scattering lengths, i.e.,

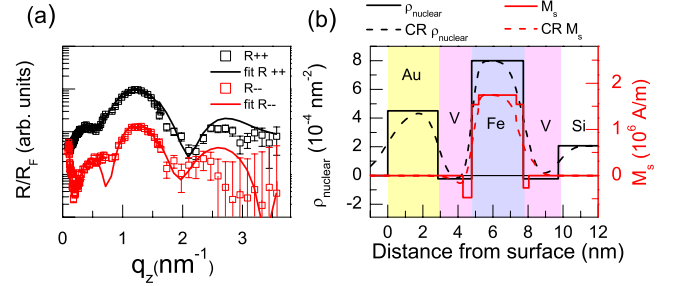


FIG. 4. (Color online) (a) Spin-up ( $R^{++}$ ) (upper curve) and spin-down ( $R^{--}$ ) (lower curve) neutron reflectometries normalized by the Fresnel reflectivity ( $R_F = 16\pi^2/q_z^4$ ) and fittings. (b) Nuclear scattering length density (SLD) and magnetization profiles considered for the fittings. Dashed lines show the convoluted roughness (CR) SLD and magnetization profiles.

$\rho = N(b \pm p)$ . The magnetic SLD  $Np$  is directly related to magnetization by the constant  $2.85 \times 10^{-12} \text{ \AA}^{-2} \text{ m/A}$ . The sign of  $p$  denotes magnetization parallel (+) or antiparallel (–) to the applied field.

The data in Fig. 4 were fitted to a model that consisted of chemical layers with the same chemistry and thicknesses obtained with the XRR analysis. To allow for magnetism in the V layer, each V layer was divided into two separate layers having the same chemistry but potentially different magnetizations. The overall thickness of each layer was constrained to remain the same as that of the corresponding layer in the XRR model. As in the case of the XRR analysis, the formalism of Parratt<sup>24,25</sup> was used to calculate the spin-dependent reflectivity curves [solid curves, Fig. 2(a)]. The  $\chi^2$  metric was optimized by perturbing the values of the magnetization in the V layers. The nuclear SLD of the constituent components was fixed to the bulk values given in the literature. The magnetic SLD of Fe was also constrained to be its bulk value. Figure 2(b) shows the nuclear SLD profile considered (continuous lines) along with the convoluted roughness SLD profile (dashed lines). The thickness and roughness values for this model are given in Table I.

In a first model, no reduction in the Fe magnetic moment at the Fe/V interfaces was included, as in the case of the XRMS analysis. V-polarized regions were found close to both Fe/V interfaces with a width of  $(0.49 \pm 0.02)$  and  $(0.32 \pm 0.05)$  nm for the upper and lower interfaces, respectively, and with magnetizations antiparallel to Fe of  $M = (-494 \pm 70.1)$  and  $(-280 \pm 122)$  kA/m, respectively. These values correspond to  $(-0.86 \pm 0.12)$  and  $(-0.48 \pm 0.21) \mu_B/\text{V}$  atom for the upper and lower interfaces, respectively. This model yields a  $\chi^2$  factor of 716. In order to further improve the fitting, reduction in the Fe magnetic moment at the Fe/V interfaces was considered, yielding a reduction in the two atomic Fe layers closest to the V layer with values of  $(1538 \pm 175)$  and  $(1542 \pm 227)$  kA/m for the upper and lower interfaces, respectively, as compared to the bulk value 1742 kA/m. In this case, the magnetic moments of the V-polarized regions slightly change to  $(-0.83 \pm 0.12)$  and  $(-0.46 \pm 0.18) \mu_B/\text{V}$  atom for the upper and lower interfaces, respectively, yielding a  $\chi^2$  factor of 711. Figure 2(b) shows the magnetization profile obtained (continuous lines) along with the convoluted roughness magnetization profile

(dashed lines). These findings are consistent with the XRMS observations. The integrated magnetization per unit area in the neutron model at RT is 4.74 mA ( $4.74 \times 10^{-4}$  emu/cm<sup>2</sup>), a value consistent with SQUID magnetometry and XRMS fittings, which after applying the obtained polarized V thicknesses corresponds to a net magnetization value of 1285 kA/m. It is worth noticing that the model that best fits our data incorporates different interfacial roughness for the upper V/Fe ( $0.29 \pm 0.03$  nm) and the lower Fe/V interfaces ( $0.60 \pm 0.02$  nm), see Table I, in agreement with the XRR refinements. Interestingly this finding is consistent with previous reports on epitaxial Fe/V superlattices, where Mössbauer studies showed that the V-on-Fe interfaces are more abrupt and less diffuse than the Fe-on-V interfaces.<sup>37</sup>

Induced V magnetic moments have been reported to be independent of the interlayer crystalline orientation between Fe and V.<sup>4</sup> Thus, our results in polycrystalline films can be compared with epitaxially grown multilayers. Our estimated value for the V magnetic moment ranging from  $-0.46$  to  $-0.86 \mu_B/V$  atom is higher than the one found in atomically flat Fe/V multilayers<sup>2</sup> ( $-0.29 \mu_B/V$  atom), where no significant roughness or interdiffusion was present and where the induced V polarization was also confined to the interface. This fact implies that moderate interfacial roughness by itself enhances the induced V magnetic moment. The polarization range of 3 ML (similar to the interface roughness), is comparable to the range found for atomically flat interfaces but here the magnitude of polarization is modified, i.e., enhanced by the roughness. Nevertheless, different V-polarization values are obtained depending on the severity of the interfacial roughness. We notice that in the case of Fe/Cr multilayers<sup>38</sup> the significant influence of interface roughness on the spin configuration of the Fe and Cr films has been reported.<sup>39,40</sup> It was found for this system that when excessive roughness is present, preferred spin alignment cannot be achieved for all pairs of spins, giving rise to frustrated coupling that in turn affects the global magnetization of the system. Similar mechanisms can help us to interpret the lower V polarization ( $-0.46 \pm 0.18 \mu_B/V$ ) observed at the bottom Fe/V interface where a severe roughness/thickness ratio of approximately 30% was measured.

#### IV. CONCLUSIONS

Structural and magnetic investigations were carried out on polycrystalline sputter-deposited V/Fe/V trilayers using x-ray nonresonant (XRR) and resonant (XRMS) reflectivity techniques, together with complementary XMCD, PNR, and SQUID measurements, in order to investigate the effect of interfacial roughness and polycrystalline microstructure on the induced polarization of V. Taken together, all the experiments indicate that V in proximity to Fe becomes magnetized with magnetization antiparallel to that of the Fe in agreement with previous reports. In the present study, the induced polarization in V was found to extend up to approximately 2–3 ML from the interface. The measured magnetic moment per V atom in the polarized area ranges from  $-0.46$  to  $-0.86 \mu_B/V$  atom, thus significantly higher than that reported for atomically flat Fe/V interfaces. The results indicate that interfacial roughness itself can enhance the induced magnetic moment of V in Fe/V interfaces due to larger contact surface at the interface, although this effect might be somewhat reduced when the roughness/thickness ratio conspires against layer integrity. These results further our understanding of proximity effects in ferromagnetic-nonmagnetic multilayered systems.

#### ACKNOWLEDGMENTS

This work was supported by NSF-DMR (Grant No. 0355171) and the Research Corporation. This work has benefited from the use of the Lujan Neutron Scattering Center at LANSCE, which is funded by the Department of Energy's Office of Basic Energy Science. Los Alamos National Laboratory is operated by Los Alamos National Security LLC under DOE Contract No. DE-AC52-06NA25396. Work at Argonne is supported by the U.S. Department of Energy, Office of Science, Office of Basic Energy Sciences, under Contract No. DE-AC-02-06CH11357. The authors also wish to acknowledge fruitful discussions with Brian Kirby from the Center for Neutron Research at NIST.

<sup>1</sup>D. Spišák and J. Hafner, Phys. Rev. B **61**, 4160 (2000).

<sup>2</sup>A. Scherz, P. Pouloupoulos, R. Nünthel, J. Lindner, H. Wende, F. Wilhelm, and K. Baberschke, Phys. Rev. B **68**, 140401(R) (2003).

<sup>3</sup>M. M. Schwickert, R. Coehoorn, M. A. Tomaz, E. Mayo, D. Lederman, W. L. O'Brien, Tao Lin, and G. R. Harp, Phys. Rev. B **57**, 13681 (1998).

<sup>4</sup>M. A. Tomaz, W. J. Antel, Jr., W. L. O'Brien, and G. R. Harp, J. Phys.: Condens. Matter **9**, L179 (1997).

<sup>5</sup>A. Scherz, H. Wende, P. Pouloupoulos, J. Lindner, K. Baberschke, P. Blomquist, R. Wäppling, F. Wilhelm, and N. B. Brookes, Phys. Rev. B **64**, 180407(R) (2001).

<sup>6</sup>K. Eftimova, A. M. Blix, B. Hjörvarsson, and P. Svedlindh, J. Phys.: Condens. Matter **14**, 12575 (2002).

<sup>7</sup>A. Scherz, H. Wende, K. Baberschke, J. Minár, D. Benea, and H. Ebert, Phys. Rev. B **66**, 184401 (2002).

<sup>8</sup>P. Isberg, B. Hjörvarsson, R. Wäppling, E. B. Svedberg, and L. Hultman, Vacuum **48**, 483 (1997).

<sup>9</sup>G. Andersson, E. Nordström, and R. Wäppling, Europhys. Lett. **60**, 731 (2002).

<sup>10</sup>X. W. Zhou and H. N. G. Wadley, J. Appl. Phys. **84**, 2301 (1998).

<sup>11</sup>G. X. Miao, A. V. Ramos, and J. S. Moodera, Phys. Rev. Lett. **101**, 137001 (2008).

<sup>12</sup>P. Bencok, S. Andrieu, P. Arcade, C. Richter, V. Ilakovac, O. Heckmann, M. Vesely, and K. Hricovini, Surf. Sci. **402-404**, 327 (1998).

<sup>13</sup>Y. Huttel, J. Avila, M. C. Asensio, P. Bencok, C. Richter, V.

- Ilakovac, O. Heckmann, and K. Hricovini, *Surf. Sci.* **402-404**, 609 (1998).
- <sup>14</sup>P. Fuchs, K. Totland, and M. Landolt, *Phys. Rev. B* **53**, 9123 (1996).
- <sup>15</sup>J. F. M. Borges, J. B. M. da Cunha, and M. I. da Costa, Jr., *J. Phys.: Condens. Matter* **15**, 1 (2003).
- <sup>16</sup>F. Stillesjo, B. Hjorvarsson, and B. Rodmacq, *J. Magn. Magn. Mater.* **126**, 102 (1993).
- <sup>17</sup>K. Obrtlík and J. Kucera, *Phys. Status Solidi A* **53**, 589 (1979).
- <sup>18</sup>S. S. P. Parkin, R. F. Marks, R. F. C. Farrow, G. R. Harp, Q. H. Lam, and R. J. Savoy, *Phys. Rev. B* **46**, 9262 (1992).
- <sup>19</sup>X. He, S.-Z. Yang, K. Tao, and Y. Fan, *Mater. Lett.* **33**, 175 (1997).
- <sup>20</sup>P. Bruno, *J. Appl. Phys.* **64**, 3153 (1988).
- <sup>21</sup>P. Bruno and J. P. Renard, *Appl. Phys. A* **49**, 499 (1989).
- <sup>22</sup>U. Köbler, *J. Phys.: Condens. Matter* **14**, 8861 (2002).
- <sup>23</sup>D. Givord, M. Rossignol, and V. M. T. S. Barthem, *J. Magn. Magn. Mater.* **258-259**, 1 (2003).
- <sup>24</sup>L. G. Parratt, *Phys. Rev.* **95**, 359 (1954).
- <sup>25</sup>L. Nevot and P. Croce, *Rev. Phys. Appl.* **15**, 761 (1980).
- <sup>26</sup>W. H. Press, B. P. Flannery, S. A. Teukolsky, and W. T. Vetterling, *Numerical Recipes in Fortran: The Art of Scientific Computation*, 2nd ed. (Cambridge University Press, Cambridge, 1992).
- <sup>27</sup><http://www.ncnr.nist.gov/resources/sldcalc.html>
- <sup>28</sup>J. B. Kortright, M. Rice, and R. Carr, *Phys. Rev. B* **51**, 10240 (1995).
- <sup>29</sup>Y. Huttel, C. Clavero, G. van der Laan, P. Bencok, T. K. Johal, J. S. Claydon, G. Armelles, and A. Cebollada, *Phys. Rev. B* **77**, 064411 (2008).
- <sup>30</sup>D. R. Lee, S. K. Sinha, D. Haskel, Y. Choi, J. C. Lang, S. A. Stepanov, and G. Srajer, *Phys. Rev. B* **68**, 224409 (2003).
- <sup>31</sup>S. K. Sinha, E. B. Sirota, S. Garoff, and H. B. Stanley, *Phys. Rev. B* **38**, 2297 (1988).
- <sup>32</sup>H. Fritzsche, Y. T. Liu, J. Hauschild, and H. Maletta, *Phys. Rev. B* **70**, 214406 (2004).
- <sup>33</sup>G. P. Felcher, R. O. Hilleke, R. K. Crawford, J. Haumann, R. Kleb, and G. Ostrowski, *Rev. Sci. Instrum.* **58**, 609 (1987).
- <sup>34</sup>C. F. Majkrzak, *Physica B* **221**, 342 (1996).
- <sup>35</sup>M. R. Fitzsimmons, S. D. Bader, J. A. Borchers, G. P. Felcher, J. K. Furdyna, A. Hoffmann, J. B. Kortright, Ivan K. Schuller, T. C. Schulthess, S. K. Sinha, M. F. Toney, D. Weller, and S. Wolf, *J. Magn. Magn. Mater.* **271**, 103 (2004).
- <sup>36</sup>M. R. Fitzsimmons and C. F. Majkrzak, in *Modern Techniques for Characterizing Magnetic Materials*, edited by Y. Zhu (Kluwer, Boston, 2005), pp. 107–152.
- <sup>37</sup>B. Kalska, P. Blomqvist, L. Häggström, and R. Wäppling, *Europhys. Lett.* **53**, 395 (2001).
- <sup>38</sup>P. Grünberg, R. Schreiber, Y. Pang, M. B. Brodsky, and H. Sowers, *Phys. Rev. Lett.* **57**, 2442 (1986).
- <sup>39</sup>D. T. Pierce, J. Unguris, R. J. Celotta, and M. D. Stiles, *J. Magn. Magn. Mater.* **200**, 290 (1999).
- <sup>40</sup>J. Unguris, R. J. Celotta, D. A. Tulchinsky, and D. T. Pierce, *J. Magn. Magn. Mater.* **198-199**, 396 (1999).